

The impact of plume rise on modelled SO₂ concentration profiles

Tereza Šedivá

Slovak hydrometeorological institute, Jeséniova 17, 833 15, Bratislava, Slovakia

tereza.sediva@gmail.com

Abstrakt

Výškové zdroje emisií, akými sú napr. priemyselné komíny, vyžadujú pri modelovaní znečistenia ovzdušia eulerovskými modelmi individuálny prístup. Zatiaľ čo pre prízemné zdroje je pre každú bunku modelu definovaná priemerná hodnota emisií, výškové zdroje potrebujeme pre správny výpočet rozptylu nečistôt uvažovať ako samostatné body s konkrétnou výškou. Dymová vlečka, ktorá sa tvorí nad výškovými zdrojmi a stúpa nahor vplyvom únikovej rýchlosti z komína a vyššej teploty emisií, môže zasahovať do viacerých vertikálnych vrstiev modelu, a tak efektívne posúva zdroj emisií do týchto vrstiev. Pre výpočet vzhnosu dymovej vlečky sa využívajú rôzne empirické metódy, ktoré sa významne líšia podľa stability atmosféry v danom čase. Preto sa vzhnos dymovej vlečky počíta v každom časovom kroku simulácie.

V tomto príspevku sa zameriavame na pochopenie algoritmu výpočtu vzhnosu dymovej vlečky modelom CMAQ a jeho stručné objasnenie. Hlavným cieľom práce je však kvantitatívne ohodnotenie významu vzhnosu dymovej vlečky pri modelovaní znečistenia ovzdušia. Tento význam skúmame porovnaním vypočítaných koncentrácií simulácie s výpočtom vzhnosu dymovej vlečky a simulácie bez tohto výpočtu. Analyzujeme koncentrácie SO₂ z dvoch výškových komínov tepelnej elektrárne Nováky. Naša analýza sa týka rozptylu emisného zdroja vplyvom vzhnosu dymovej vlečky, rozdielov koncentrácií v prízemnej vrstve modelu ako aj zmeny profilu koncentrácií vo vertikálnych vrstvách a napokon denným chodom týchto rozdielov a ich závislosťou na dennom vývoji hraničnej vrstvy atmosféry.

Anotácia

Porovnali sme simulácie rozptylu SO₂ s výpočtom vzhnosu dymovej vlečky a bez neho, za účelom kvantitatívneho ohodnotenia významu tohto výpočtu. Porovnali sme rozdiely vypočítaných koncentrácií pre prvých 8 vertikálnych modelových vrstiev a ohodnotili sme závislosť týchto rozdielov na dennom chode hraničnej vrstvy atmosféry. Taktiež sme opísali mechanizmus výpočtu vzhnosu dymovej vlečky modelom CMAQ.

Kľúčové slová: model CMAQ, modelovanie znečistenia ovzdušia, vzhnos dymovej vlečky, hraničná vrstva atmosféry.

Anotation

Two simulations of SO₂ dispersion without and with the plume rise calculation were compared with the intention to quantitatively evaluate the relevance of this calculation. The concentration differences for the first 8 vertical layers were compared and their dependence on the daily development of the boundary layer was analyzed. The mechanism of the plume rise calculation in the CMAQ model was also described.

Keywords: CMAQ model, air quality modelling, plume rise, atmospheric boundary layer.

Introduction

Meteorological situations affecting the dispersion of pollutants

Emissions in the air are carried by the atmospheric flow and therefore they obey the equations of motion of fluids. The undergoing meteorological movements of the air hence predicate dispersion of pollutants and their concentrations. Various meteorological situations have different effects on overall character of pollutant behavior. Atmospheric stability (given by the temperature profile) and wind speed are the crucial variables for estimation of dispersion situation character. In general, stable conditions suppress the intensity of turbulence in the atmosphere and hence reduce dispersion; the unstable conditions have the opposite effect.

Temperature inversion is a meteorological situation of highest significance in air quality meteorology. The inversion is stable layer with a range of effects on ground concentrations, depending on its position relative to the source. The subsequent situations are rephrased from [1].

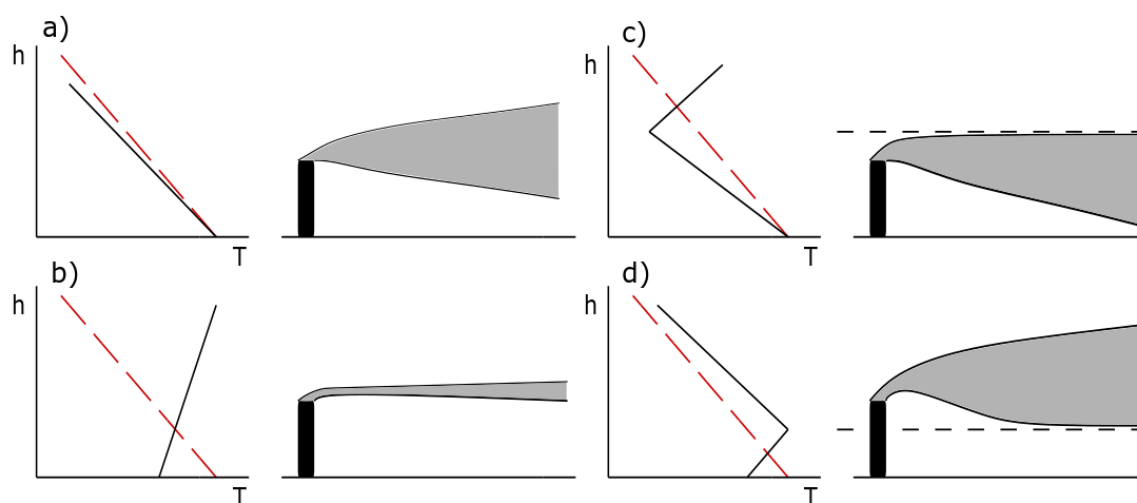


Figure 1: Plume types in various meteorological situations. In the graphs on the left, the red dashed line represents the adiabatic lapse rate of the atmosphere - $1^{\circ}\text{C}/100\text{ m}$ and the black line represent the real lapse rate of the atmosphere. Temperature inversion borderline is represented by the dashed line on the right. a) - near neutral atmosphere, b) - broad inversion, c) - inversion above the source, d) - inversion below the source.

1. Temperature inversion below the emission source

In this case, the effluent is emitted above the inversion layer (Figure 1 d)). Since the inversion layer is very stable, there is little to no turbulence within and downward mixing through the layer is very limited. Therefore, the inversion prevents the effluent to disperse into lower layers and to reach the ground. This type of temperature inversion is a favourable dispersion situation for flat areas, since the pollutants are carried over long distances above the inversion and they do not contribute to the ground level concentrations. However, it can be fairly dangerous if the source is positioned in a valley, since the hillside areas in vicinity are then prone to high concentrations episodes.

2. Temperature inversion above the emission source

The inversion layer in this case acts as a lid to pollutants trapped underneath (Figure 1 c)). This is the most unfavourable dispersion situation. It is common during the night and early morning hours, when nocturnal

stable layer is formed near the ground [2] (temperature inversion due to Earth cooling), but can be particularly significant during the wintertime, when it can last several subsequent days. In combination with increased emission output due to residential heating, this situation often yields exceeding of concentration limits. This situation is especially dangerous in partially and entirely enclosed valleys, which are strongly dependent on a right wind direction to clear the air.

3. Emission source within the temperature inversion

This situation is a combination of the previous two in its effect (Figure 1 b)). The inversion above the source prevents the effluent to disperse upwards and the inversion below to disperse downwards. As a result, the effluent spreads horizontally in the emission source height. When a strong horizontal flow is present, it can carry the pollutants to large distances. In plane areas, ground level concentrations are insignificant, however for valley-like areas the hillsides may be negatively affected as in the first case.

When inversion is not present, the pollutants are dispersed throughout the whole mixing layer evenly (in short time frame \sim hours). Higher wind speed at the top of the mixing layer partially limits the entrainment of the pollutants into the free atmosphere above, which takes several days on average. It takes 2-3 months for the pollutants to reach the tropopause [3], which separates the troposphere from the stratosphere. It is characterized by an extensive inversion layer, which acts as a lid to pollutants. It takes around 1.4 years for the air between the troposphere and stratosphere to mix.

Plume rise

When determining the height of a pollutant entering the atmosphere for high emission sources, such as industrial stacks, considering only the construction height is insufficient. The effluent has a certain escape velocity upwards when leaving the stack and its temperature is usually higher than the surrounding atmosphere, which results in positive vertical acceleration. The effective height h_e of the emission source is then determined as

$$h_e = h^* + \Delta h \quad (1)$$

where h^* is the construction height of the source and Δh is the plume rise [1]. Plume rise is defined as the difference between a height where the plume becomes passive and follows the motion of the atmospheric flow and h^* [4].

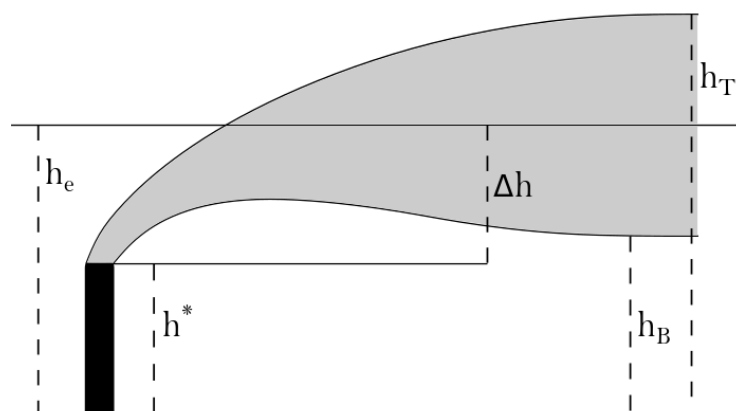


Figure 2: h^* - stack height, Δh - plume rise, h_e - effective height, h_T - plume top, h_B - plume bottom.

The plume rise is affected by the meteorological situation - mostly by atmospheric stability and wind. In an

unstable atmosphere, positive vertical currents due to convection and turbulence are prominent and as a result, the plume rise increases. On the contrary, in a stable atmosphere the turbulence is being oppressed, which results in decrease in plume rise.

Calculation of the plume rise includes many various empirical methods, which all have their strengths and weaknesses. Usually, one method of calculation is suitable only for certain meteorological situations and with different situations corrections may have to be applied or other methods are preferred.

1 The plume rise calculation in CMAQ model

Emission inputs for many Eulerian chemical-transport models, including CMAQ, do not distinguish between the individual ground level emission sources within a given grid cell. However, large point emission sources such as industrial stacks, need to be treated separately. Due to plume rise, the effective height of a source may lie several layers upward from the layer where the construction height is situated. The effective height changes with meteorological situations so it needs to be calculated systematically.

The following algorithms are mostly rephrased from the CMAQ scientific documentation [5] and the CMAQ source code. The plume rise calculation in CMAQ mostly follows the method developed by G. A. Briggs [6, 7, 8, 9]. The used method distinguishes between the rise caused by the momentum given by the escape velocity of the plume and the rise given by the buoyancy of the plume, which is caused by the density (temperature) differences between the plume and the ambient air. A key parameter for the calculation is the buoyancy flux F [$\text{m}^4 \cdot \text{s}^{-3}$] given by

$$F = \frac{1}{4} g v_e d^2 \frac{T_e - T_a}{T_e}, \quad (2)$$

where g is the gravitational acceleration, v_e is the exit velocity of the effluent from the stack, d is the inner diameter of the stack (of the effluent), T_e is the temperature of the effluent and T_a is the temperature of the ambient air at source height h^* .

When $F \leq 0$ ($T_a \geq T_e$), Δh is computed only with the momentum rise formula [10] :

$$\Delta h_m = 3d \frac{v_e}{U}, \quad (3)$$

where U is the wind speed at source height h^* .

For positive F , the plume rise is computed differently for stable, unstable and neutral conditions. The convective velocity scale H is a parameter for determination of the initial stability regime [5], defined as

$$H = g \frac{\bar{f}_s}{T_s}, \quad (4)$$

where \bar{f}_s is the mean surface heat flux and T_s is temperature at 1.5 m above the surface. Notice, that H is a parameter calculated solely using the surface parameters. Therefore, it is only a rough first approximation of the atmospheric stability. A critical value for H is equal to $H_{crit} = 3 \cdot 10^{-6} \text{ m}^2 \cdot \text{s}^{-3}$. For $H > H_{crit}$ the conditions are unstable, for $H < -H_{crit}$ the conditions are stable and neutral conditions apply for the values between.

1.1 Calculation of plume rise for stable, unstable and neutral conditions

For a stable atmosphere, the plume rise is given by [9]

$$\Delta h_s = 2.6 \left(\frac{F}{US} \right)^{1/3}, \quad (5)$$

where S is a stability parameter defined as

$$S = \max \left(\frac{g}{T_a} \frac{d\theta}{dz} \Big|_{L_s}, s \right). \quad (6)$$

The $s = 3 \cdot 10^{-5}$ parameter is a criterion for stability and $d\theta/dz|_{L_s}$ is the vertical gradient of potential temperature θ at source layer L_s .

For unstable conditions [8, 9]:

$$\Delta h_u = 30 \left(\frac{F}{U} \right)^{3/5}. \quad (7)$$

Lastly, for neutral conditions the plume rise is given as

$$\Delta h_n = \min \left[10 h^*, 1.2 \left(h^* + 1.3 \left(\frac{F}{U u_f^2} \right)^{2/5} \right) \left(\frac{F}{U u_f^2} \right)^{3/5} \right] \quad (8)$$

where u_f is a friction velocity.

Since the initial estimate of the stability is determined by the surface values, it is only an approximation. To increase the accuracy of the calculation, the plume rise is calculated for multiple stability regimes and the final value is taken as the minimum of these calculations.

A) The unstable case - $H > H_{crit}$

Since the H parameter is evaluated using the surface values of temperature and heat flux, it corresponds to the conditions in the mixing layer but it does not tell anything about the regime above. Above the mixing layer - in the free atmosphere, the turbulence basically does not exist so the free atmosphere can either be neutral or stable. Therefore, when solving for an unstable case, we need to consider mutual positioning of the source and the mixing height.

The final plume rise is determined as:

$$\Delta h = \min(\Delta h_s, \Delta h_n, \Delta h_m) \quad \text{for source above the mixing layer.} \quad (9)$$

$$\Delta h = \min(\Delta h_u, \Delta h_n, \Delta h_m) \quad \text{for source below the mixing layer.} \quad (10)$$

B) Stable case - $H < -H_{crit}$

$$\Delta h = \min(\Delta h_s, \Delta h_n) \quad \text{for stable conditions.} \quad (11)$$

C) Neutral case - $-H_{crit} < H < H_{crit}$

$$\Delta h = \Delta h_n \quad \text{for neutral conditions.} \quad (12)$$

The computed Δh was determined for the layer with the emission source. For the calculation of plume rise in the subsequent layers, we need to determine a new stability regime, which is more accurate for the following layer than the initial estimate with surface variables. We set the new stability regime depending on the used plume rise - if the final plume rise was set to stable, the new stability regime is stable as well. If the plume rise was set to the momentum rise, the next part of the algorithm (buoyancy loop) is skipped.

1.2 The buoyancy loop

The buoyancy loop computes the plume rise for the individual layers, starting with the layer of the original source h^* . For each of the following layers, the source height is set to the bottom of the current layer and a residual buoyancy flux F_r is calculated based on the stability regime determined above.

The loop initially checks whether the top of the plume exceeds the top of the current source layer L_s . If the plume rise ends in L_s , the loop is terminated. If it exceeds the top of L_s , the plume rise layer is determined as $L_p = L_s + 1$ and the residual flux F_r is calculated. F_r is used instead of F to compute the new plume rise, using the Eqs. (5), (7) and (8), where the wind speed at the original source height U is replaced by the wind speed at current L_s for each layer above the original source height h^* layer. The loop is repeated while the following condition is fulfilled:

$$h_{i+1} < h_i + \frac{3}{2}\Delta h, \quad (13)$$

where h_i and h_{i+1} are the bottom heights of the current and the upper layer, respectively and $3/2\Delta h$ is the distance between h^* and the top of the plume.

1.3 Plume fractions

As the plume rises, it also spreads to every direction according to the meteorological conditions for dispersion. The plume top and bottom can lie multiple layers apart from each other. The plume top and bottom above the ground (Figure 2) are defined as

$$h_T = h^* + \frac{3}{2}\Delta h, \quad (14)$$

$$h_B = h^* + \frac{1}{2}\Delta h. \quad (15)$$

The algorithm first finds the layers L_T and L_B where the top and bottom of the plume lie. Comparing the height of the plume in a particular layer Δh_L to the whole plume rise range, we find the fraction of the plume in the layer as

$$F_{rac}(L) = \frac{\Delta h_L}{h_T - h_B}, \quad (16)$$

where the L is arbitrary layer crossed by the plume. For the layers between the top and bottom, h_L is equal to the whole layer range. It may happen that the whole plume lies in the same layer. By fractioning the plume rise, the model evaluates the amount of the emission entering every layer.

2 Simulation specification

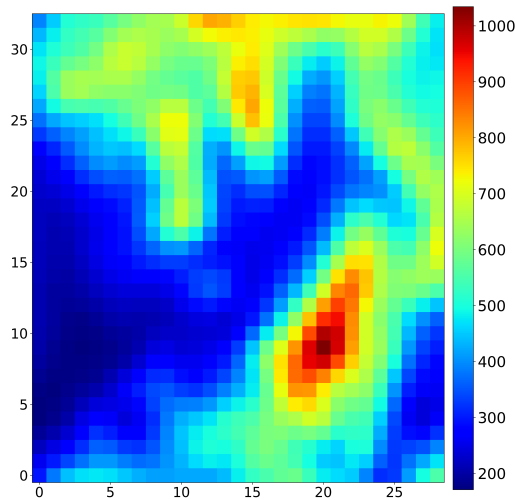


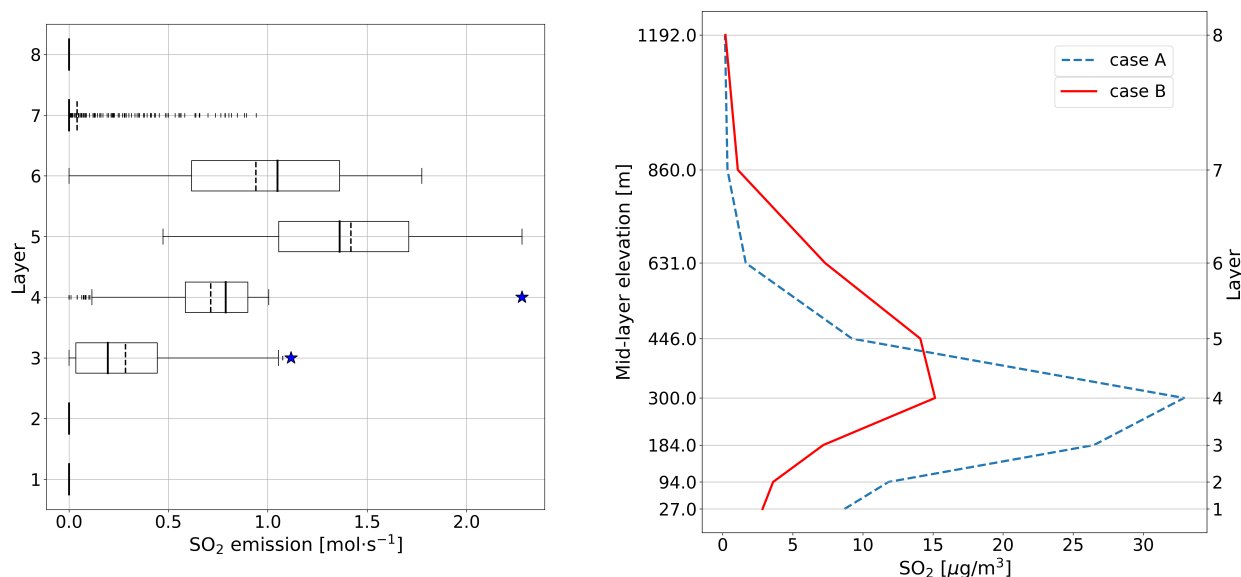
Figure 3: Terrain elevation in Nováky region [m].

CMAQ5.2 version was used for the simulation of pollutant concentrations for the period of January 1 to 30 in the Nováky region. The domain consists of 33x29 cells with resolution 1570x1570 m and 31 vertical layers. The terrain of the area is shown in Figure 3. The meteorological inputs were provided by the WRF model [11]. Since the main interest of this paper is the study of the plume rise from high emission sources, only two point emission sources are included in the simulation, which correspond to the two major stack sources from the Novaky coal-fired power station. The first stack is 150 m high, its top lying in the third vertical layer and emitting 1.12 mol/s of SO₂. The second stack is 300 m high, with the top lying in the fourth layer, emitting 2.28 mol/s of SO₂. Both stacks are situated in the same grid cell [14,16]. We only discuss SO₂ in this paper because it is the major pollutant emitted from these sources. We ran the simulation twice - with plume rise turned on and off. When the plume rise is turned off, the source becomes passive - it emits the pollutants with no exit velocity and no temperature difference, so the effluent immediately follows the atmospheric flow. Simulation was computed on SHMI's high-power computer using 32 cores.

3 Results

Our results are primarily focused on the concentration difference between the cases with the plume rise turned off (case A) and on (case B) (often referred to as without plume rise and with plume rise).

3.1 Dispersion of the emissions



(a) The dispersion of the emissions in individual layers with the plume rise. The stars represent position and magnitude of the emission source without the plume rise. The bold line within the box is a median and the dashed line is an average.

(b) Mean hourly SO₂ concentration profiles without (case A) and with (case B) plume rise in the vicinity of the source.

Figure 4

Firstly, we compared cases A and B in a context of dispersion of emissions within the vertical layers. In case A, the emissions are emitted solely in layers 3 and 4. However, in case B, the plume rise may expand between multiple layers and the plume fractioning takes place, which results in emissions dispersing from all of these

layers. The sum of the emissions over all layers stays the same, but the distribution may change significantly.

Figure 4 (a) shows a box plot of emissions within the individual layers in the source column in case B, with the stars representing the original emission magnitudes and layers. We can see that the plume rise caused a shift of the emissions to the upper layers, especially fifth and sixth. The eighth layer is not influenced by the plume rise.

Looking at concentration profiles A and B (Figure 4 (b)), we can see a large decrease near the ground and an increase for layers 5 - 7 in case B, when the plume rise is implemented. This line graph uses the mean monthly values of hourly concentration values of SO_2 in individual layers on a 5×5 grid with the source column in the middle. The y-axis shows the proportionate distances between the layers. It is apparent, that the sum of the area under (towards the y-axis) the curve B is less than under the curve A. This is caused by higher pollutant diffusion in the upper layers due to larger wind speed. Therefore, using the plume rise effectively lowers the concentrations near the ground and also lowers the overall amount of pollutants in the source vicinity.

3.2 Comparison of the surface concentration values

In this section, the surface concentrations are discussed. Figure 5 (a) shows mean hourly concentrations with the plume rise (case B) in $\mu\text{g}/\text{m}^3$. We can see that in a close vicinity of the stack, the concentrations are around $4 \mu\text{g}/\text{m}^3$. Figure 5 (b) shows the mean hourly concentration difference between the cases A and B (in this order) in the surface layer in $\mu\text{g}/\text{m}^3$. From this graph we can see that in the stack grid cell (the dark red square at [14,16]) the difference in concentration of SO_2 is more than $12 \mu\text{g}/\text{m}^3$ higher without the plume rise than with it. Comparing it to the concentrations with the plume rise on, we observe a mean 328% rise in concentration without the plume rise. This is really a significant difference in the surface concentrations. The concentration differences then decrease quickly around the source and are close to zero on majority of the domain. However, large portion of the valley still has an increase in concentration of around $5 \mu\text{g}/\text{m}^3$ with the plume rise turned off.

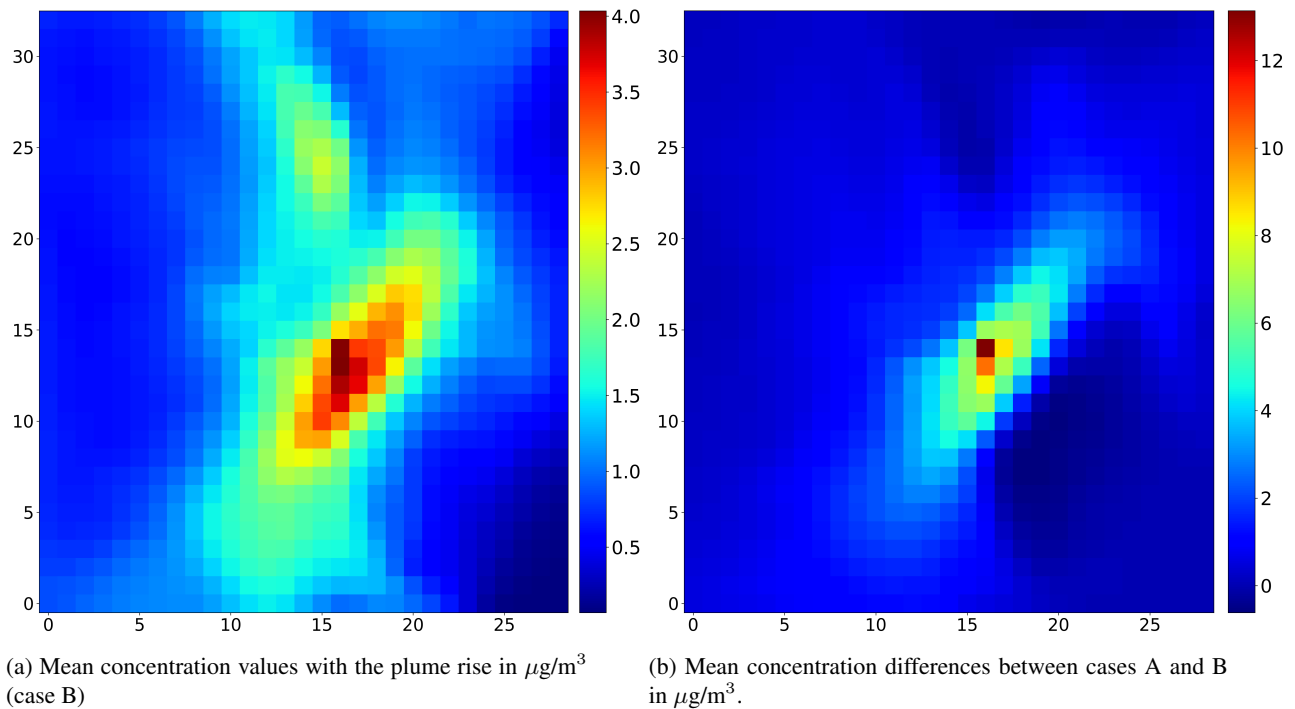


Figure 5

3.3 Daily profile of concentration differences

The plume rise depends strongly on the atmospheric stability. The stability of the boundary layer has a distinct daily regime determined by the sunshine. This regime is suppressed by the cloud cover.

During the night, a stable nocturnal layer is formed due to radiative cooling near the surface. After the sunrise, the earth begins to heat up and convective flow forms near the earth. This causes formation of the turbulence and the entrainment of the air above - the mixing layer is formed and begins to grow. It reaches its maximal depth a while after noon. After the sunset, the thermally induced turbulence stops forming, causing the mixing layer to transform into the residual layer, which lies above the stable layer and carries the residual turbulence. This daily progress has a large impact on the plume rise.

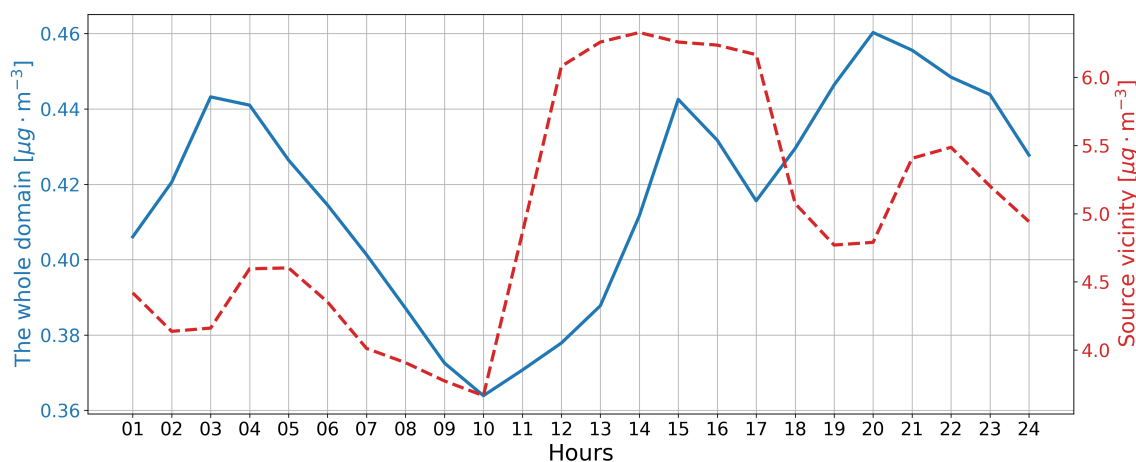


Figure 6: Mean daily profiles of concentration difference without and with plume rise of SO_2 for the whole domain - blue line (33x29 grid cells, first 8 vertical layers) and source vicinity - red dashed line (5x5 grid cells, first 8 vertical layers).

Figure 6 shows mean daily profiles of concentration differences between cases A and B for the first 8 vertical layers in $\mu\text{g}/\text{m}^3$. The left y-axis represents the mean values for the whole domain area, while the right y-axis represents the vicinity of the source (5x5 grid cells). Both profiles are always positive, which means that mean concentrations without the plume rise are higher than with the plume rise. This is expected, as the plume rise carries the pollutants in the upper layers with larger wind speed which provide better dispersion conditions. For the whole domain area the differences are below $0.5 \mu\text{g}/\text{m}^3$; but for the source vicinity the differences are substantial, reaching up to around $6 \mu\text{g}/\text{m}^3$. The following analysis is discussing the source vicinity profile.

After the sunset around 5 PM, the differences in the concentrations decrease. This is probably caused by the development of the residual layer. The residual layer is neutrally stratified with equal turbulence in all directions, resulting in equal dispersion horizontally and vertically [2] (Figure 1 a)). For that reason, whether the plume rise is present or not, the plume will disperse efficiently in all directions, reducing the differences between the two cases. During the winter this may also happen during the day, then the overcast blocks the sunlight, preventing the mixed layer to form and blend with the residual layer above.

However, we can see 2 other peaks in the profile during the night-time. The analysis of this profile from the averaged values is difficult, but it is very probable that these peaks represent the times when the stable nocturnal layer grows above the individual stacks, which have 150 m difference in height. Above the stable layer, a nocturnal jet is often formed with higher wind speeds (10-30 m/s) to balance the calm winds often present near the surface during the night [2] and therefore ensure the conservation of momentum of the atmosphere. This level with large wind speed is a probable cause of the higher concentration differences, since for the passive source it blows the pollutants rapidly right away, preventing them from reaching the higher layers as much as

within the neutrally stratified atmosphere. But the plume rise may be able to shoot a portion of the pollutants to higher layers where the residual layer with neutral stratification is still present. Once the jet moves higher with the growing stable layer, a stable regime takes place. Stable stratification then suppresses the span of the plume rise and enables slow dispersion of the pollutants, decreasing the differences between cases A and B.

We see a rapid increase in the differences after 10 AM, which is most likely linked to the rapid growth of the mixing layer once it reaches the residual layer above the stable layer. After the mixed layer is formed, various stratification regimes may occur. Each specific day has a different temperature profile and other meteorological conditions. However, in general this portion of the day is the most unstable and it is the most probable cause of this wider peak between the sunrise and sunset to show in the average.

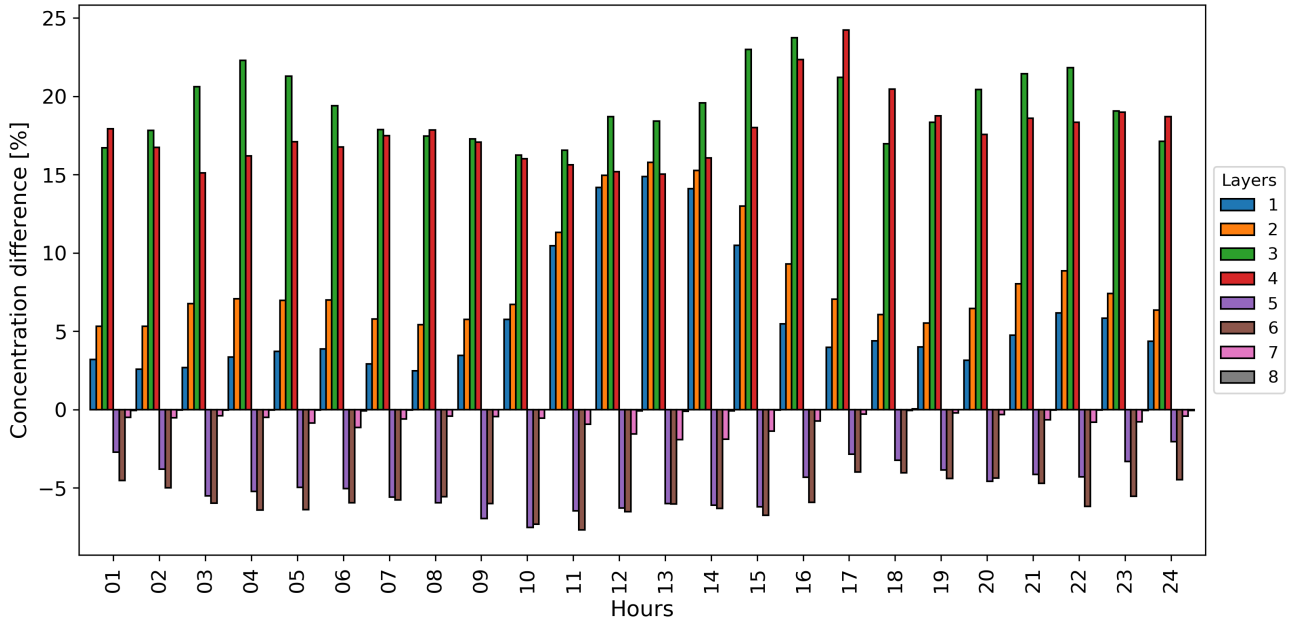


Figure 7: Mean daily profiles of concentration differences for individual layers without and with plume rise for the source vicinity (5x5 grid cells).

In Figure 7, the daily profiles of concentration differences in the individual layers are shown in the source vicinity (5x5 grid cells). Coefficient of variation ν (standard deviation normalized by the average) is a convenient indicator of the daily variation. For each layer, they are summarized in Table 1.

Table 1: Coefficients of variance for concentration differences in individual layers

Layer	ν	Layer	ν
1	0.65	5	0.29
2	0.39	6	0.18
3	0.11	7	0.66
4	0.12	8	0.99

We can see, that first, seventh, and eighth layers show the highest variance throughout the day. In these layers with higher variance, the concentration differences are more dependent on the meteorological situation. For example, with an inversion above the source the surface layer will have much higher concentrations than with the inversion below the source, when the surface concentrations might be negligible. In the third and fourth

layers the concentration differences are more stable in value simply because they contain the emission sources at all times. The fifth layer has higher variance than the third and fourth layer, because it is the layer mostly affected by the plume rise. Similarly, second layer is the one mostly affected by the downward mixing of pollutants. The stability of concentration differences in the sixth layer is probably caused by similar dispersion to this layer whether the plume rise is present or not.

Figure 7 also shows the 3 peaks discussed for Figure 6. We can see that for the first 4 layers, the afternoon peak is shifted gradually towards the right for the subsequent layers. This supports our theory of large concentration differences being dependent on the formation of the mixing layer.

The peak of the third layer at 10 PM is accompanied with smaller peaks in the first and second layers, which start to rise around 1-2 hours after. The peak of the third layer at 4 AM probably rises due to higher concentration from the upper stack without the plume rise after the stable layer grows above it, compared to the concentrations with the plume rise which would be smaller since a portion of the pollutants would be shot into the fifth and sixth layers, which can also be seen in their profiles in the Figure 7. This supports our theory of the stable layer crossing the stacks consecutively.

Conclusion

Our aim in this paper was to compare the results of two otherwise identical air quality simulations with the plume rise option turned on and off. The simulation was computed with the chemical transport model CMAQ version 5.2 in the domain covering the Nováky city and surrounding mountains with resolution of 1570x1570 m. The emission sources consisted of two stacks of 150 m and 300 m heights, which lay in the third and fourth layers in the same column of the domain. The secondary aim was to understand and intelligibly formulate the theoretical mechanism of plume rise calculation in the CMAQ model.

The theory

Since the documentation of the CMAQ model does not describe the algorithm of plume rise calculation sufficiently, we compared several resources, but we primarily followed the algorithm straight from the CMAQ source code. We focused on the main points which are the different methods used to compute the plume rise at different stability regimes as well as the overall principle of the mechanism. The mechanism consists of the initial determination of the plume height evaluated with surface values, the calculation of the plume rise in subsequent layers above the stack until the plume rise does not exceed the next layer, and fractioning of the plume rise into the individual layers.

Results of the simulation

We compared the results of the simulation without and with plume rise in multiple categories. First, we analyzed the dispersion of the emission sources due to plume rise (Figure 4 (a)). The original emission sources were placed in layers 3 and 4 and the plume rise highly affected layers 5 and 6. The seventh layer was affected in less than 50% of cases and layer 8 was unaffected by the plume rise. The resulting changes in the concentration profiles with the plume rise on (Figure 4 (b)) show lowered concentrations near the surface, higher concentrations in layers 5 to 7 and overall smaller sum of pollutant mass in the domain, which is caused by larger wind speed in the upper layers carrying the pollutants out of the domain faster.

The analysis of the surface level concentrations (Figure 5) show that the mean surface concentration within the grid cell with the stack is 328% (around $12 \mu\text{g}/\text{m}^3$) higher with the plume rise turned off. For a large portion of the valley the concentrations are around $5 \mu\text{g}/\text{m}^3$ higher without the plume rise.

The average daily variation of the concentration differences was analyzed (Figure 6). A close dependency of the concentration differences on the boundary layer daily regime was observed. This includes processes of a growth of the mixing layer, its transformation into residual layer and a growth of the stable nocturnal layer. The daily profile shows one wide peak between the sunset and sunrise which is most likely caused by the on-average unstable regime of the atmosphere during these hours. Interestingly, the profile shows 2 more peaks during the night-time. These two additional peaks are most likely caused by growth of the stable layer above the stacks successively. Our theory on the concentration difference peaks was supported by daily profiles of the individual layers, where we were able to observe the development of the surface layer height during the day.

The variance of the concentration differences was evaluated with the coefficients of variation (Table 1). The layers 3 and 4, which contain the emission sources at all times, showed the smallest variation during the day. Layers 1,7,8 showed the highest variance, since the concentrations in these layers are more strongly affected by the meteorological phenomena.

In our future work, we would like to take the daily profiles of concentration differences for specific days and analyze them with the corresponding meteorology (temperature and wind profiles, overcast). We are also planning to run the simulation again, but with only one stack, which should help us to understand the daily concentration differences profile better.

References

- [1] Bednář, Jan- Zikmunda, Otakar, 1984: Fyzika mezní vrstvy atmosféry, Academia nakladatelství Československé akademie věd, Praha.
- [2] Stull, Roland B., 1988: An Introduction to Boundary Layer Meteorology, University of Wisconsin, Madison, U.S.A.
- [3] Závodský, D.- Ďurec, F.- Medved', M., 2001: Atmospheric Chemistry and Air Pollution Modelling, Matej Bel University, Banská Bystrica.
- [4] Seinfeld, John H.- Pandis, Spyros N., 2006: Atmospheric chemistry and physics: from air pollution to climate change, 2nd Edition, John Wiley Sons, New York.
- [5] Byun, D W.- J.K S. Ching., 1999: SCIENCE ALGORITHMS OF THE EPA MODELS-3 COMMUNITY MULTISCALE AIR QUALITY (CMAQ) MODELING SYSTEM. U.S. Environmental Protection Agency, Washington, D.C., EPA/600/R-99/030 (NTIS PB2000-100561).
- [6] Briggs, Gary A., 1971: Some Recent Analyses of Plume Rise Observation, pp. 1029-1032 in Proceedings of the Second International Clean Air Congress, edited by H. M. Englun and W. T. Beery. Academic Press, New York.
- [7] Briggs, Gary A., 1972: Discussion on Chimney Plumes in Neutral and Stable Surroundings, Atmos. Environ. 6, 507-510.
- [8] Briggs, G.A., 1983 communication: Plume rise equations used in EPA models. Meteorology Division, Environmental Sciences Research Lab.; Research Triangle Park, NC.
- [9] Briggs, G.A., 1984.: Plume Rise and Buoyancy Effects. In: Atmospheric Science and Power Production, D.R. Anderson, Ed., DOEITIC-27601 (DE84005177), Technical Information Center, U.S. DOE, Oak Ridge, TN, 850 pp.
- [10] Turner, D.B., 1985: Proposed Pragmatic Methods for Estimating Plume Rise and Plume Penetration through Atmospheric Layers. Atmos. Environ., 19, 1215-1218.

-
- [11] Skamarock, W. C.- Klemp J. B.-Dudhia J.-Gill D. O.-Barker D. M.-Duda M. G.- Huang X. Y.- Wang W.- Powers J. G., 2008, A Description of the Advanced Research WRF Version 3. NCAR Tech. Note NCAR/TN-475+STR, 113 pp. doi:10.5065/D68S4MVH.